SLAC–PUB–7868
ICHEP–PA08 #180
July 1998

Measurement of the B^+ and B^0 Lifetimes using Topological Vertexing at SLD *

The SLD Collaboration**
Stanford Linear Accelerator Center,
Stanford University, Stanford, CA 94309

Abstract

The lifetimes of B^+ and B^0 mesons have been measured using a sample of 400,000 hadronic Z^0 decays collected by the SLD experiment at the SLC between 1993 and 1998. This inclusive topological measurement includes 250,000 hadronic Z^0 decays collected since 1996 with the SLD upgrade vertex detector. A high statistics sample of 30028 (19636) charged (neutral) vertices with good charge purity is obtained. The charge purity is enhanced by using the vertex mass, the SLC electron beam polarization (63% for 1993, 77% for 1994-6 and 73% for 1997-8) and an opposite hemisphere jet charge technique. Lifetime fits for the full data sample yield the following preliminary results: $\tau_{B^+} = 1.686 \pm 0.025(\text{stat}) \pm 0.042(\text{syst})$ ps, $\tau_{B^0} = 1.589 \pm 0.026(\text{stat}) \pm 0.055(\text{syst})$ ps, $\tau_{B^+}/\tau_{B^0} = 1.061 \pm^{0.031}_{0.029} (\text{stat}) \pm 0.027(\text{syst})$.

Paper Contributed to the XXIXth International Conference on High Energy Physics, July 23-29, 1998, Vancouver, Canada.

*Work supported in part by the Department of Energy contract DE–AC03–76SF00515.

The spectator model predicts that the lifetime of a heavy hadron depends upon the properties of the constituent weakly decaying heavy quark Q and is independent of the remaining, or spectator, quarks in the hadron. This model fails for the charm hadron system for which the lifetime hierarchy $\tau_{D^+} \sim 2\tau_{D_s^+} \sim 2.5\tau_{D^0} \sim 5\tau_{\Lambda_c^+}$ is observed. Since corrections to the spectator model are predicted to scale with $1/m_Q^2$ the B meson lifetimes are expected to differ by less than 10% [1]. Hence a measurement of the B^+ and B^0 lifetimes provides a test of this prediction. In addition, the specific B meson lifetimes are needed to determine the element V_{cb} of the CKM matrix.

The analysis is performed on the 1993-5 data sample of 150,000 hadronic Z^0 decays collected with the original vertex detector VXD2 together with 250,000 hadronic Z^0 decays collected using the upgrade vertex detector VXD3 [2] by SLD at the SLC. The excellent 3-D vertexing capabilities of SLD are exploited with an inclusive topological vertexing technique [3] to identify B hadron vertices produced in hadronic Z^0 decays with high efficiency. The decay length is measured using the reconstructed vertex location while the B hadron charge is determined from the total charge of the tracks associated with the vertex. This inclusive technique has the advantage of very efficient B vertex reconstruction since most B decays are used. The new measurement presented here is an update of previously reported results [4].

The components of the SLD utilized by this analysis are the Central Drift Chamber (CDC)[5] for charged track reconstruction and momentum measurement and the CCD pixel Vertex Detector (VXD)[2, 5] for precise position measurements near the interaction point. These systems are immersed in the 0.6 T field of the SLD solenoid. Charged tracks reconstructed in the CDC are linked with pixel clusters in the VXD by extrapolating each track and selecting the best set of associated clusters[5]. For a typical charged particle from the primary vertex or heavy hadron decay, the total efficiency of reconstruction in the CDC and linking to VXD hits is $\sim 96\%$ within the VXD acceptance. For VXD2 the track impact parameter resolutions at high momentum are 11 μm and 38 μm in the $r\phi$ and rz projections respectively (z points along the beam direction), while multiple scattering contributions are $70\,\mu\text{m}\,/(p\sin^{3/2}\theta)$ in both projections (where the momentum p is expressed in GeV/c). For VXD3 the track impact parameter resolutions at high momentum are 11 μm and 23 μm in the $r\phi$ and rz projections while multiple scattering contributions are $40\,\mu\text{m}\,/(p\sin^{3/2}\theta)$ in both projections.

The centroid of the micron-sized SLC Interaction Point (IP) in the $r\phi$

plane is reconstructed with a measured precision of $\sigma_{IP} = (5 \pm 2)\,\mu$m using tracks in sets of ~ 30 sequential hadronic Z^0 decays. The median z position of tracks at their point of closest approach to the IP in the $r\phi$ plane is used to determine the z position of the Z^0 primary vertex on an event-by-event basis. A precision of $\sim 52\,\mu$m [5] ($\sim 32\,\mu$m) on this quantity is estimated using $Z^0 \to b\overline{b}$ Monte Carlo simulation for VXD2 (VXD3).

The simulated $Z^0 \to q\,\overline{q}$ events are generated using JETSET 7.4 [6]. The B meson decays are simulated using the CLEO B decay model [7] tuned to reproduce the spectra and multiplicities of charmed hadrons, pions, kaons, protons and leptons as measured at the Υ(4S) by ARGUS and CLEO [8]. The branching fractions of the charm hadrons are tuned to the existing measurements [9]. The B mesons and baryons are generated with lifetimes of $\tau_{B^+} = 1.64$ ps, $\tau_{B^0} = 1.55$ ps, $\tau_{B^0_s} = 1.57$ ps, and $\tau_{\Lambda_b} = 1.22$ ps. The b-quark fragmentation follows the Peterson *et al.* parameterization [10]. The SLD detector is simulated using GEANT 3.21 [11].

Hadronic Z^0 event selection requires at least 7 CDC tracks which pass within 5 cm of the IP in z at the point of closest approach to the beam and which have momentum transverse to the beam direction p_T >200 MeV/c. The sum of the energy of the charged tracks passing these cuts must be greater than 18 GeV. These requirements remove background from $Z^0 \to l^+l^-$ events and two-photon interactions. In addition, the thrust axis determined from energy clusters in the calorimeter must have $|\cos\theta| < 0.71$, (< 0.85 for VXD3) within the acceptance of the vertex detector. These requirements yield a sample of $\sim 250,000$ hadronic Z^0 decays.

Due to the extra tracking information provided by the upgrade vertex detector, track quality cuts are looser for the VXD3 data. Good quality tracks used for vertex finding must have a CDC hit at a radius<39 cm, and have $\geq$40 ($\geq$23 for VXD3) hits to insure that the lever arm provided by the CDC is appreciable. The CDC tracks must have p_T >400 MeV/c (p_T >250 MeV/c for VXD3) and extrapolate to within 1 cm of the IP in $r\phi$ and within 1.5 cm in z to eliminate tracks which arise from interaction with the detector material. The fit of the track must satisfy χ^2/d.o.f.< 5 (< 8 for VXD3). At least one (two for VXD3) good VXD link is required, and the combined CDC/VXD fit must also satisfy χ^2/d.o.f.< 5 (< 8 for VXD3).

The topological vertex reconstruction is applied separately to the tracks in each hemisphere (defined with respect to the event thrust axis). The vertexing algorithm is described in detail in Ref. [3] and summarized here.

The vertices are reconstructed in 3-D coordinate space by defining a vertex function $V(\mathbf{r})$ at each position $\mathbf{r}$. The helix parameters for each track i are used to describe the 3-D track trajectory as a Gaussian tube $f_i(\mathbf{r})$, where the width of the tube is the uncertainty in the measured track location close to the IP. A function $f_0(\mathbf{r})$ is used to describe the location and uncertainty of the IP. $V(\mathbf{r})$ is defined as a function of $f_0(\mathbf{r})$ and the $f_i(\mathbf{r})$ such that it is small in regions where fewer than two tracks (required for a vertex) have significant $f_i(\mathbf{r})$, and large in regions of high track multiplicity. Maxima are found in $V(\mathbf{r})$ and clustered into resolved spatial regions. Tracks are associated with these regions to form a set of topological vertices.

The efficiency for reconstructing at least one secondary vertex in a b hemisphere is $\sim 50\%$ ($\sim 67\%$) for VXD2 (VXD3). The efficiency falls at shorter decay length as it becomes harder to resolve the secondary vertex from the IP. For hemispheres containing secondary vertices, the 'seed' vertex is chosen to be the one with the highest $V(\mathbf{r})$ value. Vertices consistent with a $K_s^0 \to \pi^+\pi^-$ decay, within a 14 MeV invariant mass window, are excluded from the seed vertex selection and the two tracks are discarded.

A vertex axis is formed by a straight line joining the IP to the seed vertex. The 3-D distance of closest approach of a track to the vertex axis, T, and the distance from the IP along the vertex axis to this point, L, are calculated for all quality tracks. Monte Carlo studies show that tracks which are not directly associated with the seed vertex but which pass T$<$ 0.1 cm and L/D$>$ 0.3 (where D is the distance from the IP to the seed vertex) are more likely to have been produced by the B decay sequence than to have an alternative origin. Hence such tracks are added to the set of tracks in the seed vertex to form the candidate B decay vertex, containing tracks from both the B and cascade D decays. This set of tracks is fitted to a common vertex. If the probability of the vertex fit is greater than 5% the B decay location is taken to be the fitted vertex location. Since the vertex includes tracks form both the B and cascade charm decay points the fit probability distribution is not flat and 47% (55%) of vertices reconstructed with VXD2 (VXD3) have a fit probability below 5%. The reconstruction of the B decay location in this case is improved by dividing the tracks (if there are at least three) into two 'sub-vertices' by selecting the combination of tracks with maximum two sub-vertex fit probability. The B decay location is given by the sub-vertex closest to the IP, reducing systematic dependence upon the physics of the $B \to D$ decay. The distance from the IP to the B decay location is the reconstructed

decay length. Since the purity of the B charge reconstruction is lower for decays close to the IP, where tracks are more likely to be wrongly assigned, decay lengths are required to be > 1 mm. To avoid using the vertices of tracks originating from interactions with the detector material, the distance of the decay vertex from the beamline is required to be < 24 mm for VXD2 (< 22 mm for VXD3), i.e. more than 1 mm inside the SLC beampipe.

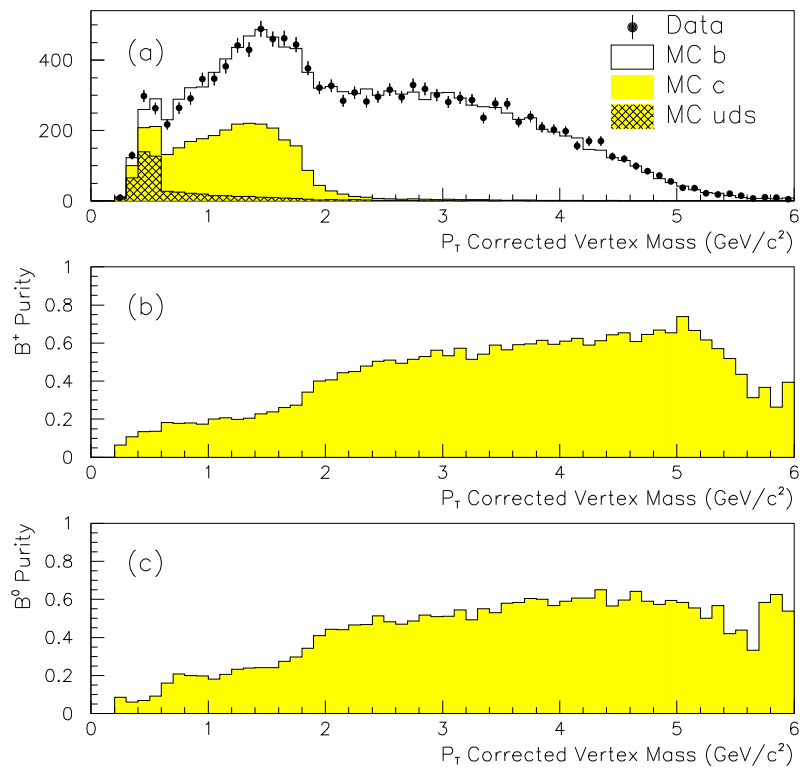

Figure 1: (a) M_{P_T} of reconstructed vertex for 1996 VXD3 data (points) and Monte Carlo (histogram), (b) B^+ fraction in the charged sample, (c) B^0 fraction in the neutral sample.

The mass M of the reconstructed vertex is calculated by assuming each track has the mass of a pion. The transverse component P_T of the total momentum of vertex tracks relative to the vertex axis is calculated in order to determine the P_T corrected mass:

$$M_{P_T} = \sqrt{M^2 + P_T^2} + |P_T|. \tag{1}$$

This quantity is the minimum mass the decaying hadron could have in order to produce a vertex with the quantities M and P_T. The direction of the vertex axis is varied within the 1σ limits constraining the axis at the measured IP and reconstructed seed vertex such that the P_T is minimized within this variation. This procedure prevents non-B background vertices acquiring a high M_{P_T} due to a fluctuation in the measured P_T. The accurate 3-D vertexing and precisely measured IP at SLD allow significant gain in the b-tag efficiency with high purity using this technique [12].

A comparison of the distribution of M_{P_T} in data and Monte Carlo is shown in Fig. 1(a). Vertices from K_s^0 decays surviving the K_s^0 rejection can be seen around 0.5 GeV/c^2. This figure shows that a large fraction of the charm and light flavor contamination in the sample is eliminated by requiring $M_{P_T} > 2$ GeV/c^2. It is also required that $M_{P_T} < 5.2$ GeV/c^2 since vertices with M_{P_T} greater than the B meson mass are likely to contain background tracks. These cuts yield a sample with b hemisphere purity of $\sim 98\%$ with an efficiency of 30% (38%) for VXD2 (VXD3). The average B decay vertex multiplicity is 4.5 tracks.

To improve the B hadron charge reconstruction, tracks which fail the initial selection but have $p_T > 200$ MeV/c and $\sqrt{\sigma_{r\phi}^2 + \sigma_{rz}^2} < 700\,\mu$m, where $\sigma_{r\phi}$ (σ_{rz}) is the uncertainty in the track position in the $r\phi$ (rz) plane close to the IP, are considered as decay track candidates. The charge of these tracks which pass the cuts T$<$ 0.1 cm and L/D$>$ 0.3 is added to the B decay charge. On average, 0.5 tracks pass these criteria in b hemispheres. These lower quality tracks are used only to improve the charge reconstruction.

Fig. 2 shows a comparison of the reconstructed charge between data and Monte Carlo for (a) VXD2 and (b) VXD3 (1996 only). At this stage the charged sample consists of 8676 (21352) vertices with vertex charge equal to $\pm$ 1,2 or 3, while the neutral sample consists of 5197 (14439) vertices with charge equal to 0 for VXD2 (VXD3) data. Monte Carlo studies indicate that for VXD2 (VXD3) the charged sample is 97.0% (97.6%)pure in B hadrons consisting of 52.4% (55.1%) B^+, 33.8% (32.0%) B^0, 9.1% (8.6%) B_s^0, and 4.7% (4.3%) B baryons. (Charge conjugation is implied throughout this paper with the exception of the notation B_+ and B_- introduced later to distinguish the charged mesons $B(\overline{b}u)$ and $B(b\overline{u})$ and respectively.) Similarly, the neutral sample is 97.9% (98.2%)pure in B hadrons consisting of 26.8% (24.1%) B^+, 52.4% (54.1%) B^0, 14.2% (15.0%) B_s^0 and 6.6% (6.8%)

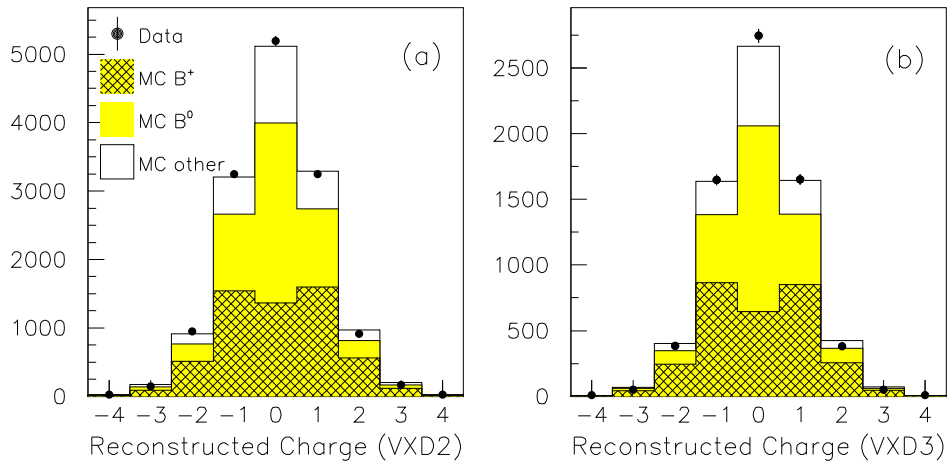

Figure 2: Reconstructed vertex charge for data (points) and Monte Carlo (histogram) for (a) 1993-5 and (b) 1996.

B baryons. The statistical precision of the measurement depends on the separation between the B^+ and B^0 in these samples.

The lifetime measurement relies on the ability to separate B^+ and B^0 decays by making use of the vertex charge. Monte Carlo studies show that the purity of the charge reconstruction is more likely to be eroded by losing tracks from the B decay chain through track selection inefficiencies and track mis-assignment than by gaining mis-assigned tracks originating from the primary or other background to the B decay. Furthermore, the decays which are missing some B tracks tend to have lower vertex mass as well as lower charge purity. Fig. 1(b) and (c) show the fraction of B^+ decays in the charged sample and the fraction of B^0 decays in the neutral sample respectively for VXD3 MC. The probability for the vertex to originate from a positively charged, neutral or negatively charged B meson is denoted as $P_c(B_+)$, $P_c(B^0)$ and $P_c(B_-)$ respectively, normalized such that $P_c(B_+) + P_c(B^0) + P_c(B_-) = 1$. Vertices are given a weight, w, according to their analyzing power for separating B^+ and B^0 decays: $w = |2P_c(B^+) - 1|$, where $P_c(B^+) = P_c(B_+) + P_c(B_-)$. The probabilities, and hence the weight, are a function of M_{P_T}.

The charge reconstruction in Fig. 2 shows good agreement between data and MC. A further check is made using the SLC electron beam polarization. The polarized forward-backward asymmetry $A_{FB}(P_e, \cos\theta)$ can be described

by

$$A_{FB}(P_e, \cos\theta) = 2A_b \, \frac{A_e - P_e}{1 - A_e P_e} \, \frac{\cos\theta}{1 + \cos^2\theta} \, , \tag{2}$$

where $A_b = 0.94$ and $A_e = 0.155$ (Standard Model values), P_e is the electron beam longitudinal polarization, and θ is the angle between the thrust axis and the electron beam direction (the thrust axis is signed such that it points in the same hemisphere as the reconstructed vertex). Using negative (positive) vertex charge, with vertices weighted by the M_{P_T} dependent analyzing power, to tag the b ($\overline{b}$) quark flavor the resulting forward backward asymmetry is sensitive to the accuracy of the vertex charge reconstruction. Good agreement between data and MC can be seen in Fig. 3 for the 1997-8 data, indicating that the MC adequately reproduces the charge reconstruction purity of the data. (Random vertex charge assignment would generate distributions with no signed $\cos\theta$ asymmetry.)

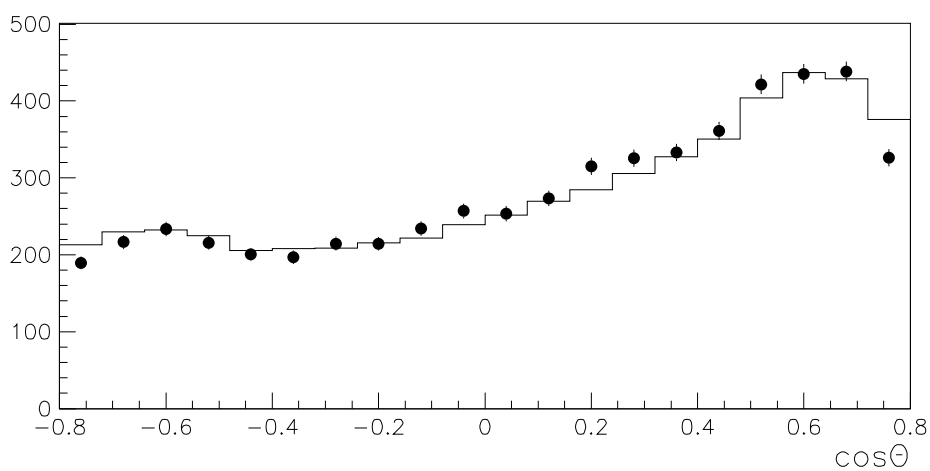

Figure 3: Distribution of cosθ signed by ($P_e \times$ vertex charge) for 1997-8 data (points) and Monte Carlo (histogram).

The polarized forward-backward asymmetry can be used to tag the initial state b or $\overline{b}$ flavor of the hemisphere. The initial state $b/\overline{b}$ tag is also used to enhance the charged sample purity by giving a higher (lower) weight to the B^+ hypothesis if the vertex charge agrees (disagrees) with the $b/\overline{b}$ tag. The probability for correctly tagging a b quark at production using the e^- beam polarization is expressed as

$$P_A(b) = \frac{1 + A_{FB}(P_e, \cos\theta)}{2} \ . \tag{3}$$

A jet charge technique is used in addition to the polarized forward-backward asymmetry. For this tag, tracks in the hemisphere opposite that of the reconstructed vertex are selected. These tracks are required to have momentum transverse to the beam axis $p_\perp > 150$ MeV/c, total momentum $p < 50$ GeV/c, impact parameter in the plane perpendicular to the beam axis $\delta < 2$ cm, distance between the primary vertex and the track at the point of closest approach along the beam axis $\Delta z < 10$ cm, and $|\cos\theta| < 0.8$ (<0.87 for VXD3). With these tracks, an opposite hemisphere momentum-weighted track charge is defined as

$$Q_{opp} = \sum_i q_i \left|\vec{p}_i \cdot \hat{T}\right|^\kappa \ , \tag{4}$$

where q_i is the electric charge of track i, $\vec{p}_i$ its momentum vector, $\hat{T}$ is the thrust axis direction, and κ is a coefficient chosen to be 0.5 to maximize the separation between b and $\overline{b}$ quarks. The probability for correctly tagging a b quark in the initial state of the vertex hemisphere can be parameterized as

$$P_Q(b) = \frac{1}{1 + e^{\alpha Q_{opp}}} \ , \tag{5}$$

where the coefficient $\alpha = -0.27$ as determined using the Monte Carlo simulation. This technique is independent of the polarized forward-backward asymmetry tag. The average purity of the $b/\overline{b}$ tag is 72% using the forward backward asymmetry ($|P_e| = 77\%$) and 67% for the jet charge technique.

The two initial state tags can be combined to form an overall initial state tag with $b/\overline{b}$ quark probability $P_i(b)/P_i(\overline{b})$ (a function of P_e, $\cos\theta$ and Q_{opp}). This probability is then combined with that obtained from the vertex charge reconstruction (a function of M_{P_T}) to determine the overall probability of a B^+ or B^0 decay:

$$P(B^+) = \frac{P_c(B_+)P_i(\overline{b}) + P_c(B_-)P_i(b)}{P_c(B_+)P_i(\overline{b}) + P_c(B_-)P_i(b) + 0.5 \times P_c(B^0)} \tag{6}$$

where B_+ and B_- denote the positively and negatively charged B mesons separately and $P(B^0) = 1 - P(B^+)$. If the probability $P(B^+) > P(B^0)$ the vertex is classified as charged, otherwise it is added to the neutral sample.

In either case it is weighted by the analyzing power $w = |2P(B^+) - 1|$. Including the initial state tag information enhances the statistical power of the analysis by $\sim$20%.

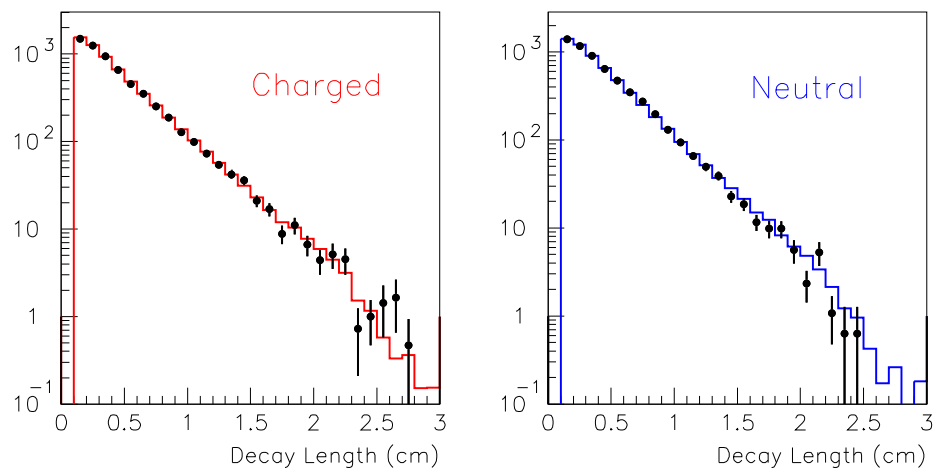

Figure 4: Decay length distributions for 1997-8 data (points) and best fit Monte Carlo (histogram).

The B^+ and B^0 lifetimes are extracted from the decay length distributions of the B vertices in the charged and neutral samples using a binned χ^2 fit. These distributions are fitted simultaneously to determine the B^+ and B^0 lifetimes. For each set of parameter values, Monte Carlo decay length distributions are obtained by reweighting entries from generated B^+ and B^0 decays in the original Monte Carlo decay length distributions with $W(t,\tau) = \left(\frac{1}{\tau}\, e^{-t/\tau}\right) / \left(\frac{1}{\tau_{gen}}\, e^{-t/\tau_{gen}}\right)$, where τ is the desired B^+ or B^0 lifetime, τ_{gen} is the average lifetime generated in the Monte Carlo, and t is the proper time of each decay. The fit then compares the decay length distributions from the data with the reweighted Monte Carlo distributions. The two parameter fit to the 1993-5 data yields lifetimes of $\tau_{B^+} = 1.724 \pm 0.051$ ps and $\tau_{B^0} = 1.567 \pm 0.055$ ps, with a ratio of $\tau_{B^+}/\tau_{B^0} = 1.100^{+0.068}_{-0.064}$ and a combined χ^2/d.o.f. $= 87.8/76$. The fit to the smaller 1996 VXD3 data sample yields lifetimes of $\tau_{B^+} = 1.654 \pm 0.066$ ps and $\tau_{B^0} = 1.603 \pm 0.069$ ps, with a ratio of $\tau_{B^+}/\tau_{B^0} = 1.032^{+0.081}_{-0.075}$ and a χ^2/d.o.f. $= 79.3/76$. The fit to the 1997-8 VXD3 data sample yields lifetimes of $\tau_{B^+} = 1.678 \pm 0.031$ ps and $\tau_{B^0} = 1.591 \pm 0.032$ ps, with a ratio of $\tau_{B^+}/\tau_{B^0} = 1.055^{+0.038}_{-0.036}$ and a χ^2/d.o.f.

= 92.0/76. Fig. 4 shows the reconstructed decay length for data and best fit MC for the 1997-8 data and the charged and neutral samples. (The fits are made using histograms in which the bin size increases with decay length such that the number of entries per bin remains approximately constant.)

Several checks of the analysis were performed. The lifetimes were extracted in four separate detector regions: four azimuthal angle regions and four polar angle regions. The measured lifetimes in these regions were found to be consistent with one another. The vertex charge distribution for the data was found to agree with the simulation in different decay length regions, indicating that the slight decay length dependence of the charge reconstruction purity is well-modeled.

Table 1 summarizes the systematic errors on the B^+ and B^0 lifetimes and their ratio. The systematics are determined separately for the 1993-5, 1996 and 1997-8 measurements and then combined taking into account correlated uncertainties. To account for a discrepancy between data and Monte Carlo in the fraction of tracks passing the selection criteria, a 4% tracking efficiency correction with dependence on track momenta and angles is applied to the simulation [5]. The corrected Monte Carlo is used in the lifetime fits, with the effect of the entire correction taken as the systematic error. The uncertainty due to tracking resolution for VXD2, mainly due to remaining vertex detector misalignments in the rz plane, is estimated by applying to the Monte Carlo track rz impact parameter ϕ dependent systematic shifts of up to 20 μm and a random Gaussian smear with $\sigma = 20\mu\mathrm{m}/\sin\theta$. Smearing is also applied to the VXD3 MC in order to reproduce the tracking resolution observed in the data. The total effect of this correction is again assigned as a systematic error.

The physics modeling systematic uncertainties were determined as follows. The mean fragmentation energy $< x_E >$ of the B hadron [13] and the shape of the x_E distribution [14] were varied. Since the fragmentation is assumed to be identical for the B^+ and B^0 mesons, this uncertainty has little effect on the lifetime ratio. The four branching fractions for $B^+/B^0 \to \overline{D^0}/D^- X$ were varied by twice the uncertainty given in Ref. [15] for $B \to \overline{D^0}/D^- X$. The fraction of B^+/B^0 decays producing a $D\overline{D}$ pair was also varied. The average B^+ and B^0 decay multiplicity was varied by ± 0.3 tracks [16] in an anticorrelated manner. Uncertainties in the B_s^0 and B baryon lifetimes and production fractions mostly affect the B^0 lifetime since the neutral B_s^0 and B baryon are a more significant background for the B^0

decays. The results are corrected to correspond to a B_s^0 (B baryon) lifetime

Table 1: Summary of systematic uncertainties in the B^+ and B^0 lifetimes and their ratio for the combined 1993-8 data.

Systematic Error		$\Delta\tau_{B^+}$ (ps)	$\Delta\tau_{B^0}$ (ps)	$\Delta\frac{\tau_{B^+}}{\tau_{B^0}}$
	Detector Modeling			
Tracking efficiency		0.005	0.011	0.008
Tracking resolution		0.003	0.003	0.003
	Physics Modeling			
b fragmentation	0.700 ± 0.011	0.035	0.035	$<.003$
	x_E shape	0.008	0.012	$<.003$
BR($B \to DX$)		0.006	0.008	0.006
BR($B \to D\overline{D}X$)	0.18 ± 0.05	0.010	0.009	0.011
B decay multiplicity	5.3 ± 0.3	0.003	0.004	0.003
B_s^0 fraction	0.115 ± 0.040	0.008	$<.003$	0.005
B baryon fraction	0.072 ± 0.040	0.012	0.029	0.013
B_s^0 lifetime	1.49 ± 0.06 ps	$<.003$	0.014	0.009
B baryon lifetime	1.22 ± 0.05 ps	$<.003$	0.005	0.003
D decay multiplicity		0.005	0.005	0.006
D decay K^0 yield		0.003	0.011	0.008
	Monte Carlo and Fitting			
Fitting systematics		0.008	0.010	0.009
MC statistics		0.005	0.006	0.007
TOTAL		0.042	0.055	0.027

of 1.49 (1.22) ps. The systematic errors due to uncertainties in charmed meson decay topology were estimated by changing the Monte Carlo D decay charged multiplicity and K^0 production according to the uncertainties in experimental measurements [17]. The effect of varying the lifetime of charm hadrons (D^+, D^0, D_s, Λ_c), as well as their momentum spectra in the B decay rest frame was found to be negligible.

The fitting uncertainties were determined by varying the bin size used in

the decay length distributions, and by modifying the cuts on the minimum decay length (no cut–2 mm) and maximum radius cuts (20 mm–no cut) used in the fit. Fit results are consistent within statistics for these variations, but a systematic error is conservatively assigned using the RMS variation of the results.

In summary, from 400,000 Z^0 decays collected by SLD between 1993 and 1998, the B^+ and B^0 lifetimes have been measured using an inclusive topological technique. The analysis isolates 49,664 B hadron candidates with good charge purity enhanced by the vertex mass, e^- beam polarization and opposite hemisphere jet charge information. The combined 1993-8 measurements yield the following preliminary results:

$$\begin{aligned}
\tau_{B^+} &= 1.686 \pm 0.025(\text{stat}) \pm 0.042(\text{syst})\ \text{ps}, \\
\tau_{B^0} &= 1.589 \pm 0.026(\text{stat}) \pm 0.055(\text{syst})\ \text{ps}, \\
\frac{\tau_{B^+}}{\tau_{B^0}} &= 1.061 \pm^{0.031}_{0.029}\ (\text{stat}) \pm 0.027(\text{syst}).
\end{aligned}$$

These results are consistent with the expectation that the B^+ lifetime is up to 10% greater than that of the B^0 and have the best statistical accuracy among current measurements [18].

We thank the personnel of the SLAC accelerator department and the technical staffs of our collaborating institutions for their outstanding efforts.

References

[1] see for example, I.I. Bigi *et al.*, in *B Decays*, edited by S. Stone (World Scientific, New York, 1994), p. 132.

[2] K. Abe *et al.*, Nucl. Inst. and Meth. **A400**, 287 (1997).

[3] D. J. Jackson, Nucl. Inst. and Meth. **A388**, 247 (1997).

[4] K. Abe *et al.*, Phys. Rev. Lett. **79**, 590 (1997).

[5] K. Abe *et al.*, Phys. Rev. **D53**, 1023 (1996).

[6] T. Sjöstrand, Comp. Phys. Comm. **82**, 74 (1994).

[7] CLEO B decay model provided by P. Kim and the CLEO Collaboration.

[8] B. Barish *et al.*, Phys. Rev. Lett. **76**, 1570 (1996); H. Albrecht *et al.*, Z. Phys. **C58**, 191 (1993); H. Albrecht *et al.*, Z. Phys. **C62**, 371 (1994); P. Avery *et al.*, CLEO CONF 96-28, July 1996; L. Gibbons *et al.*, Phys. Rev. **D56**, 3783 (1997); T.E. Coan *et al.*, CLNS 97/1516; CLEO Collab., CLEO CONF 97-27, Aug. 1997; M. Zoeller, Ph.D. Thesis, SUNY Albany, 1994; X. Fu *et al.*, Phys. Rev. Lett. **79**, 3125 (1997); D. Gibaut *et al.*, Phys. Rev. **D53**, 4734 (1996).

[9] Particle Data Group, Phys. Rev. **D54**, Part I (1996).

[10] C. Peterson *et al.*, Phys. Rev. **D27**, 105 (1983).

[11] R. Brun *et al.*, Report No. CERN-DD/EE/84-1, 1989.

[12] K. Abe *et al.*, Phys. Rev. Lett. **80**, 660 (1998).

[13] see for example, R. Akers *et al.*, Z. Phys. **C60**, 601 (1993); D. Buskulic *et al.*, Z. Phys. **C62**, 179 (1994); P. Abreu *et al.*, Z. Phys. **C66**, 323 (1995).

[14] M. G. Bowler, Z. Phys. **C11**, 169 (1981).

[15] F. Muheim, in *Proceedings of the 8th Meeting Division of Particles and Fields, Albuquerque, August, 1994* (World Scientific, New York, 1995), Vol. 1, p. 851.

[16] H.Albrecht *et al.*, Z. Phys. **C54**, 13 (1992); R.Giles *et al.*, Phys. Rev. **D30**, 2279 (1984).

[17] D.Coffman *et al.*, Phys. Lett. **B263**, 135 (1991).

[18] D. Buskulic *et al.*, Z. Phys. **C71**, 31 (1996); P. Abreu *et al.*, Z. Phys. **C68**, 13 (1995); P. Abreu *et al.*, Report No. CERN-PPE/96-139, (1996); W. Adam *et al.*, Z. Phys. **C68**, 363 (1995); R. Akers *et al.*, Z. Phys. **C67**, 379 (1995); F. Abe *et al.*, FERMILAB-Pub-98/167-E, June 1998; W. Adam *et al.*, Z. Phys. **C68**, 363 (1995); F. Abe *et al.*, Phys. Rev. Lett. **72**, 3456 (1994).

**List of Authors

K. Abe,[2] K. Abe,[19] T. Abe,[27] I.Adam,[27] T. Akagi,[27] N. J. Allen,[4] A. Arodzero,[20] W.W. Ash,[27] D. Aston,[27] K.G. Baird,[15] C. Baltay,[37] H.R. Band,[36] M.B. Barakat,[14] O. Bardon,[17] T.L. Barklow,[27] J.M. Bauer,[16] G. Bellodi,[21] R. Ben-David,[37] A.C. Benvenuti,[3] G.M. Bilei,[23] D. Bisello,[22] G. Blaylock,[15] J.R. Bogart,[27] B. Bolen,[16] G.R. Bower,[27] J. E. Brau,[20] M. Breidenbach,[27] W.M. Bugg,[30] D. Burke,[27] T.H. Burnett,[35] P.N. Burrows,[21] A. Calcaterra,[11] D.O. Caldwell,[32] D. Calloway,[27] B. Camanzi,[10] M. Carpinelli,[24] R. Cassell,[27] R. Castaldi,[24] A. Castro,[22] M. Cavalli-Sforza,[33] A. Chou,[27] E. Church,[35] H.O. Cohn,[30] J.A. Coller,[5] M.R. Convery,[27] V. Cook,[35] R. Cotton,[4] R.F. Cowan,[17] D.G. Coyne,[33] G. Crawford,[27] C.J.S. Damerell,[25] M. N. Danielson,[7] M. Daoudi,[27] N. de Groot,[27] R. Dell'Orso,[23] P.J. Dervan,[4] R. de Sangro,[11] M. Dima,[9] A. D'Oliveira,[6] D.N. Dong,[17] P.Y.C. Du,[30] R. Dubois,[27] B.I. Eisenstein,[12] V. Eschenburg,[16] E. Etzion,[36] S. Fahey,[7] D. Falciai,[11] C. Fan,[7] J.P. Fernandez,[33] M.J. Fero,[17] K.Flood,[15] R. Frey,[20] T. Gillman,[25] G. Gladding,[12] S. Gonzalez,[17] E.L. Hart,[30] J.L. Harton,[9] A. Hasan,[4] K. Hasuko,[31] S. J. Hedges,[5] S.S. Hertzbach,[15] M.D. Hildreth,[27] J. Huber,[20] M.E. Huffer,[27] E.W. Hughes,[27] X.Huynh,[27] H. Hwang,[20] M. Iwasaki,[20] D. J. Jackson,[25] P. Jacques,[26] J.A. Jaros,[27] Z.Y. Jiang,[27] A.S. Johnson,[27] J.R. Johnson,[36] R.A. Johnson,[6] T. Junk,[27] R. Kajikawa,[19] M. Kalelkar,[26] Y. Kamyshkov,[30] H.J. Kang,[26] I. Karliner,[12] H. Kawahara,[27] Y. D. Kim,[28] R. King,[27] M.E. King,[27] R.R. Kofler,[15] N.M. Krishna,[7] R.S. Kroeger,[16] M. Langston,[20] A. Lath,[17] D.W.G. Leith,[27] V. Lia,[17] C.-J. S. Lin,[27] X. Liu,[33] M.X. Liu,[37] M. Loreti,[22] A. Lu,[32] H.L. Lynch,[27] J. Ma,[35] G. Mancinelli,[26] S. Manly,[37] G. Mantovani,[23] T.W. Markiewicz,[27] T. Maruyama,[27] H. Masuda,[27] E. Mazzucato,[10] A.K. McKemey,[4] B.T. Meadows,[6] G. Menegatti,[10] R. Messner,[27] P.M. Mockett,[35] K.C. Moffeit,[27] T.B. Moore,[37] M.Morii,[27] D. Muller,[27] V.Murzin,[18] T. Nagamine,[31] S. Narita,[31] U. Nauenberg,[7] H. Neal,[27] M. Nussbaum,[6] N.Oishi,[19] D. Onoprienko,[30] L.S. Osborne,[17] R.S. Panvini,[34] H. Park,[20] C. H. Park,[29] T.J. Pavel,[27] I. Peruzzi,[11] M. Piccolo,[11] L. Piemontese,[10] E. Pieroni,[24] K.T. Pitts,[20] R.J. Plano,[26] R. Prepost,[36] C.Y. Prescott,[27] G.D. Punkar,[27] J. Quigley,[17] B.N. Ratcliff,[27] T.W. Reeves,[34] J. Reidy,[16]

P.L. Reinertsen,[33] P.E. Rensing,[27] L.S. Rochester,[27] P.C. Rowson,[8] J.J. Russell,[27] O.H. Saxton,[27] T. Schalk,[33] R.H. Schindler,[27] B.A. Schumm,[33] J. Schwiening,[27] S. Sen,[37] V.V. Serbo,[36] M.H. Shaevitz,[8] J.T. Shank,[5] G. Shapiro,[13] D.J. Sherden,[27] K. D. Shmakov,[30] C. Simopoulos,[27] N.B. Sinev,[20] S.R. Smith,[27] M. B. Smy,[9] J.A. Snyder,[37] H. Staengle,[9] A. Stahl,[27] P. Stamer,[26] R. Steiner,[1] H. Steiner,[13] M.G. Strauss,[15] D. Su,[27] F. Suekane,[31] A. Sugiyama,[19] S. Suzuki,[19] M. Swartz,[27] A. Szumilo,[35] T. Takahashi,[27] F.E. Taylor,[17] J. Thom,[27] E. Torrence,[17] N. K. Toumbas,[27] A.I. Trandafir,[15] J.D. Turk,[37] T. Usher,[27] C. Vannini,[24] J. Va'vra,[27] E. Vella,[27] J.P. Venuti,[34] R. Verdier,[17] P.G. Verdini,[24] S.R. Wagner,[27] D. L. Wagner,[7] A.P. Waite,[27] Walston, S.,[20] J.Wang,[27] C. Ward,[4] S.J. Watts,[4] A.W. Weidemann,[30] E. R. Weiss,[35] J.S. Whitaker,[5] S.L. White,[30] F.J. Wickens,[25] B. Williams,[7] D.C. Williams,[17] S.H. Williams,[27] S. Willocq,[27] R.J. Wilson,[9] W.J. Wisniewski,[27] J. L. Wittlin,[15] M. Woods,[27] G.B. Word,[34] T.R. Wright,[36] J. Wyss,[22] R.K. Yamamoto,[17] J.M. Yamartino,[17] X. Yang,[20] J. Yashima,[31] S.J. Yellin,[32] C.C. Young,[27] H. Yuta,[2] G. Zapalac,[36] R.W. Zdarko,[27] J. Zhou.[20]

(The SLD Collaboration)

[1] *Adelphi University, South Avenue- Garden City,NY 11530,*
[2] *Aomori University, 2-3-1 Kohata, Aomori City, 030 Japan,*
[3] *INFN Sezione di Bologna, Via Irnerio 46 I-40126 Bologna, Italy,*
[4] *Brunel University, Uxbridge, Middlesex - UB8 3PH United Kingdom,*
[5] *Boston University, 590 Commonwealth Ave. - Boston,MA 02215,*
[6] *University of Cincinnati, Cincinnati,OH 45221,*
[7] *University of Colorado, Campus Box 390 - Boulder,CO 80309,*
[8] *Columbia University, Nevis Laboratories P.O.Box 137 - Irvington,NY 10533,*
[9] *Colorado State University, Ft. Collins,CO 80523,*
[10] *INFN Sezione di Ferrara, Via Paradiso,12 - I-44100 Ferrara, Italy,*
[11] *Lab. Nazionali di Frascati, Casella Postale 13 I-00044 Frascati, Italy,*
[12] *University of Illinois, 1110 West Green St. Urbana,IL 61801,*
[13] *Lawrence Berkeley Laboratory, Dept.of Physics 50B-5211 University of California- Berkeley, CA 94720,*
[14] *Louisiana Technical University, Dept. of Physics, Ruston, LA 71272,*
[15] *University of Massachusetts, Amherst,MA 01003,*

[16] *University of Mississippi, University,MS 38677,*
[17] *Massachusetts Institute of Technology, 77 Massachusetts Avenue Cambridge, MA 02139,*
[18] *Moscow State University, Institute of Nuclear Physics 119899 Moscow, Russia,*
[19] *Nagoya University, Nagoya 464 Japan,*
[20] *University of Oregon, Department of Physics Eugene,OR 97403,*
[21] *Oxford University, Oxford, OX1 3RH, United Kingdom,*
[22] *Universita di Padova, Via F. Marzolo,8 I-35100 Padova, Italy,*
[23] *Universita di Perugia, Sezione INFN, Via A. Pascoli I-06100 Perugia, Italy,*
[24] *INFN, Sezione di Pisa, Via Livornese,582/AS Piero a Grado I-56010 Pisa, Italy,*
[25] *Rutherford Appleton Laboratory, Chiton,Didcot - Oxon OX11 0QX United Kingdom,*
[26] *Rutgers University, Serin Physics Labs Piscataway,NJ 08855-0849,*
[27] *Stanford Linear Accelerator Center, 2575 Sand Hill Road Menlo Park,CA 94025,*
[28] *Sogang University, Ricci Hall Seoul, Korea,*
[29] *Soongsil University, Dongjakgu Sangdo 5 dong 1-1 Seoul, Korea 156-743,*
[30] *University of Tennessee, 401 A.H. Nielsen Physics Blg. - Knoxville, Tennessee 37996-1200,*
[31] *Tohoku University, Bubble Chamber Lab. - Aramaki - Sendai 980, Japan,*
[32] *U.C. Santa Barbara, 3019 Broida Hall Santa Barbara,CA 93106,*
[33] *U.C. Santa Cruz, Santa Cruz,CA 95064,*
[34] *Vanderbilt University, Stevenson Center,Room 5333 P.O.Box 1807,Station B Nashville,TN 37235,*
[35] *University of Washington, Seattle,WA 98105,*
[36] *University of Wisconsin, 1150 University Avenue Madison,WS 53706,*
[37] *Yale University, 5th Floor Gibbs Lab. - P.O.Box 208121 - New Haven,CT 06520-8121.*